

Analysis of global buckling of FRP pipes under axial compression

Peng Feng, Peng Qian, & Lieping Ye

Department of Civil Engineering, MOE Key Laboratory of Structural Engineering and Vibration, Tsinghua University, Beijing, China

ABSTRACT: Fiber reinforced polymer (FRP) is suitable for structures in corrosive environment and long-span light-weight structures due to its high-strength, light-weight, and anti-corrosive qualities. The buckling behavior of pultruded fiber reinforced polymer pipes, which are always under the axial forces as the members of long-span lattice structures, was investigated by axial compressive loading tests. Twelve long pipes specimens in four groups with different slenderness ratios were loaded to buckle. And the ultimate compressive strength of the GFRP pipe was obtained by the tests of short pipes. Based on results of the tests and literature, a formula of the buckling load of FRP pipes under axially compressive load was obtained by fitting the available experimental data, in which the initial defect and the eccentricity are considered. It well predicts the buckling failure load GFRP pipe under axial compression.

1 INTRODUCTION

Fiber reinforced polymer (FRP) has been promoted and applied gradually in various fields of the modern engineering since the 1940s due to its characteristic of high-strength, high-modulus ratio, and anti-corrosive. The price of FRPs has decreased for the progress of manufacturing technology and industrialization, which has brought more application in civil engineering structures since the 1970s (Ye&Feng 2006; Shen 1996). GFRP (glass FRP), CFRP(carbon FRP), and AFRP(aramid FRP) are FRPs in common use, and GFRP is in the broadest application in engineering due to its reasonable price and larger ratio of elongation (Shen 1996; Zhang 2003; Berthelog 1999).

FRP with the characteristic of light-weight and high-strength which is the ideal material to build long-span spatial structures can form lots of lattice structure such as grid and net shell. It has lots of advantages for building large-span special roof such as the good adjustability for structures, the ability to form variously shaped spatial curves, the convenience to transport and install, low-cost for maintenance, well-durability, short-construction cycle, and the ability to avoid corrosion induced by rain and dew. The behavior of pultruded GFRP pipes, which are the members of spatial grid structure, under axial compression was investigated in tests. The axial bearing capacity and basic material parameters of the GFRP pipes were first obtained through short-pipe compressive test; then long pipes under axial compression were tested to study the relations between its stability and slenderness ratio and its instability failure modes; the approach to calculate the buckling load of under axially compressed pipes is presented on the basis of study and summarization of the result of the test and literature.

2 SHORT PIPES STRENGTH TESTS

The tested GFRP pipes made from E-glass fiber and vinyl resin was produced by pultrusion, with circle section with external diameter of 41.2mm and thickness of 3.6mm. Axially compressive tests to short pipes with length of 120mm were processed to obtain material properties and

the axially compressive strength. Five specimens were taken from different batches of the GFRP pipe products. The GFRP pipes were exerted axial pressure after alignment on compressive test machine. Strain gauges were placed in the opposed places of the central section of the outer-surface of the pipes to measure the axial strain and transverse strain of the GFRP pipes.

Table 1 Experimental result of short GFRP pipes under axial compression

No.	Failure load P_u (kN)	Longitudinal failure strains $\varepsilon_{u,L}$ ($\mu\varepsilon$)	Transverse failure strains $\varepsilon_{u,T}$ ($\mu\varepsilon$)	Failure stress $\sigma_{u,L}$ (MPa)	Longitudinal elastic modulus E_L (MPa)	Poisson's ratio ν_T
SCGP-1	92.0	7819	2936	216.4	27682	0.39
SCGP-2	71.0	6192	2178	166.8	27054	0.35
SCGP-3	87.0	7284	3463	204.4	28347	0.38
SCGP-4	73.0	6331	1709	171.6	21626	0.27
SCGP-5	87.0	7820	2480	204.4	26404	0.35
Average	84.3	7279	2764	198.4	27372	0.37

* SCGP-4 is discarded because it was crushed under eccentric load for sliding equipment.

The relations of the load and strain measured during the progression of the tests were linear in the gross. A sound of “pipa” was caught when the longitudinal strain reached to 5000 $\mu\varepsilon$, and the sound continued to the destruction of the pipe. The longitudinal strain of the pipe reached to 6200 $\mu\varepsilon$ to 7800 $\mu\varepsilon$ when the specimens were destructed which was a sudden course comparatively and accompanied by huge noises. Finally, a number of longitudinal cracks appeared on GFRP pipes. The experimental results were presented in Table.1, in which the mechanical properties were taken from the average value of the pipes.

3 LONG PIPES STABILITY TESTS

Four groups of GFRP pipes with the different slenderness ratios and the same cross-section as the tested short pipes, each group including three same specimens, were tested to investigate the stability of GFRP pipes under axial compression. Their parameters are shown in Table 2. The GFRP pipes were placed in the fixture (the effective calculated length of element includes the height of the fixture with two ends), then were exerted longitudinal pressure after alignment. The loading was controlled by force. The longitudinal strain and lateral displacements of the middle section, and vertical displacement at the load end were measured, the testing setup and the placement of the strain gauge and displacement meters as shown in Figure 1 and Figure 2.

Table 2 Geometrical parameters of tested long GFRP pipes

No.	Length l (mm)	Slenderness ratio λ	Support condition
LCGP35	700	35	Fixed ends
LCGP45	1000	45	Fixed ends
LCGP55	1300	55	Fixed ends
LCGP90	1500	90	Fixed bottom / hinged top

*LCGP35: Long Compressive GFRP Pipes 35 (slenderness ratio)

The tested specimens had the similar phenomenon in the gross: little deformation at the beginning of the loading; when it closed to buckling load, the lateral displacement in the central part of the bar increased rapidly; then the buckling of the whole element occurred. The lateral deformation of the pipes was in the shape of half-wave sine curve when it was instability. All belong to the global buckling failure.

Figure 3 shows the axial force-middle-point lateral displacement curves of all groups of specimens. It can be seen in the curves that the existing of the initial defect leads the lateral displacement increasing with the load raising, and there appears a distinctive inflexion with the buckling, since then the vertical load nearly become invariable but the lateral deformation increases rapidly until the failure of the sample. Figure.3(a) shows the axial force-lateral displacement curves of LCGP35 group. As the existence of a small gap in the support bracket,

there is an inflexion on the curves at the beginning of the loading. The lateral displacement of LCGP35-1 and LCGP35-3 increased rapidly after instability, and the specimens reached to the ultimate compression and failure occurred when the lateral displacement reached to 10mm; the LCGP35-2 appeared failure soon after instability as the stress concentration near the end, and the lateral displacement was only 4mm at this point. Figure 5(b) shows the axial force-lateral displacement curves of LCGP45 group. The lateral stiffness of LCGP45-3 had an abrupt change because a contact slip happened when the load reached to 10kN. The stiffness of three specimens kept homologous until the instability of the samples. Among them, the buckling load of LCGP45-1 was comparatively lower, 44kN, as the inadequately end constraint caused by little rotation of the fixture, but the buckling loads of the other two were around 60kN. Figure 5(c) shows the axial force-lateral displacement curves of LCGP55 group. The lateral stiffness of LCGP55-3 increased slowly before its buckling, and it had the largest buckling load in the three specimens, which proved that its initial defect is comparatively small. Obviously, the initial defect is a very important factor to influence the buckling load of elements. Figure 5(d) shows the axial force-lateral displacement curves of LCGP90 group. When LCGP90-1 was loaded to 8kN, the ends of the bar were pressure-compacted partially, so its stiffness bounced suddenly, that is its lateral displacement kept constant while the axial load increased. To 13kN, the lateral displacement increased suddenly, it went to the condition of instability quickly. Compared with LCGP90-1, the stiffness of the other two specimens changed little during the loading.

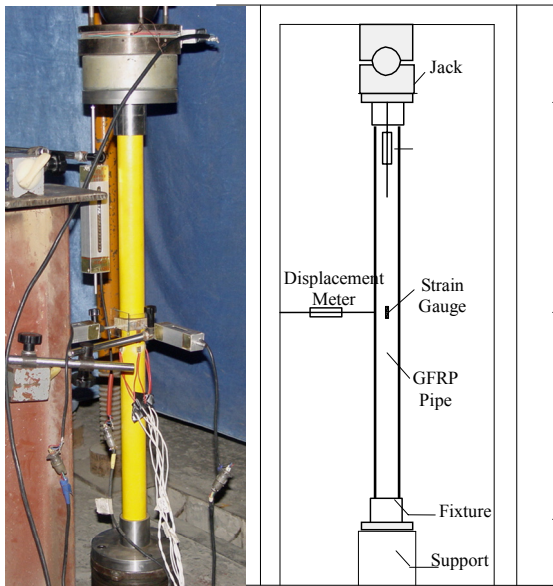


Figure 1. Testing setup for long GFRP pipes under axial compression

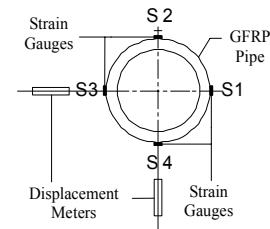


Figure 2. Location of measured points in the middle section

4 OVERALL STABILITY ANALYSIS OF GFRP PIPES

There are a few researches on the overall stability of GFRP members published. Goodman et al (1969) tested three boron/epoxy FRP pipes with the radius of 81mm and the thickness of 0.53mm under axial compression. The ratio between the experimental results and the calculated result by the Euler formula, Eq.(1), are 0.81, 0.97 and 1.06 respectively. The elastic modulus E was determined by experiment of short column under axial compression.

$$P_E = \frac{\pi^2 EI}{L^2} \quad (1)$$

Hewson et al (1978) investigated the flexural buckling, torsional buckling and flexural torsional coupling buckling of pultruded C-shaped GFRP members under axial compression. The flexural buckling load of the components was calculated by Euler formula, but E and G were replaced

by longitudinal elastic modulus E_L determined by bending test and longitudinal-transversal shear modulus G_{LT} determined through torsion test. The error of the buckling loads of experiment to the theoretical result was from 5% to 11%. Lee and Hewson (1978) found that the shear deformation must be considered as E_L/G_{LT} was comparatively large based on the study on the buckling properties of the CFRP C-shaped members under axial compression in 1979. They suggested that the buckling load of slender FRP component should be calculated by the modified Euler formula as

$$P_t = \frac{P_E}{1 + (P_E / K_s A_g G_{lt})} \quad (2)$$

where P_E is the Euler buckling load determined by Eq.(1), A_g is the net section area of the FRP member, and K_s is the shear parameters related to the shape of the cross section, for rectangular section and circular section which is 0.83 and 0.9 respectively. Zureick et al (1992;1997) had an experimental study on GFRP square pipes under axial compression. The section of the specimens was a 76.2mm×76.2mm square with the wall of thickness of 6.3mm. Their slenderness ratio were 89,87,76, and 66 respectively. It was found that the buckling load of the experimental results corresponded well with the results of the modified Euler formula, Eq.(2). Zureick and Scott (1997) conducted experimental studies on two types of wide flange H-shaped section and 2 types of box-section GFRP components under axial compression. Each type of section included 6 specimens, totally 24 specimens. Their effective slenderness ratio were from 36 to 103. The ratios between the experimental results and the calculated results by Eq.(1) and Eq.(2) are 0.85-0.97 and 0.88-1.01 respectively. Hence, the reduction factor of 0.85 on the basis of the buckling load by Eq.(2) was proposed for design of GFRP component under axial compression. Barbero et al (1993; 1994) studied the buckling properties of the FRP components under the coupling influence of global buckling and local buckling.

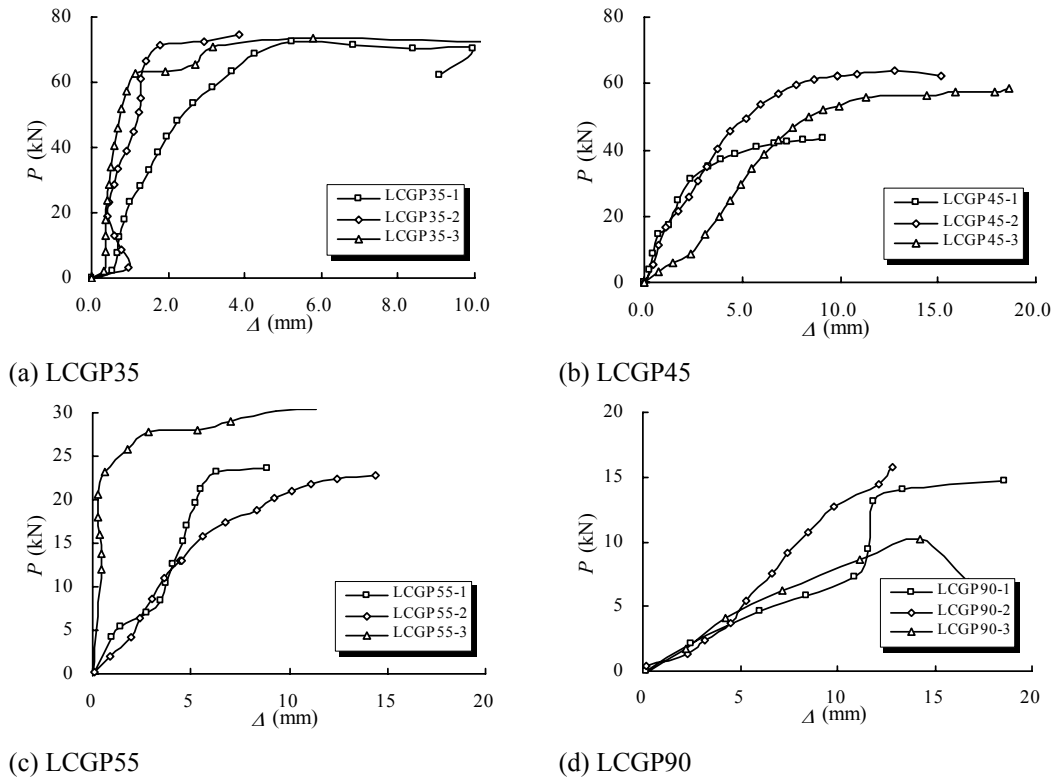


Figure 3 Axial force-lateral displacement curves of tested pipes

It can be seen that the influence of initial geometric defect and initial eccentricity were not considered in the above formulas of the buckling load of FRP members under axial compression. But it is certain that the initial geometric defect and initial eccentricity exist in real struc-

tures for different reasons. Therefore, a modified Perry formula (Chen 2003) to calculate the buckling load of the GFRP member is suggested based on fitting tested members to obtain the equivalently relatively initial bending ε_0 . The formula is

$$\varphi = \frac{1}{2\bar{\lambda}^2} [(1 + \varepsilon_0 + \bar{\lambda}^2) - \sqrt{(1 + \varepsilon_0 + \bar{\lambda}^2)^2 - 4\bar{\lambda}^2}] \quad (3)$$

$$P_{er} = \varphi f_L A$$

where the φ is stability factor, P_{er} is the buckling load, f_L is the longitudinal compressive strength, which should be 198.4MPa for GFRP pipes used according to the experimental result in Table 1, and $\bar{\lambda}$ is the regularized slenderness ratio, which is :

$$\bar{\lambda} = \frac{\lambda}{\pi} \sqrt{\frac{f_L}{E_L}}$$

$$\lambda = \frac{\mu L}{r} \quad r = \sqrt{\frac{I}{A}} \quad (4)$$

where E_L is the longitudinal elastic modulus of the GFRP component, I is the sectional moment of inertia, A is the section area of components, r is the sectional gyration radius, and μ is the effective length coefficient of the component.

Refer to The Technical Code of Cold-Formed Thin-Wall Steel Structures (2001) , the expression of initially relative eccentric ratio is

$$\varepsilon_0 = a + b\bar{\lambda}^2 \quad (5)$$

Fitting the data in this test and literature (Zureick 1992; 1997), 32 specimens totally, using the least square method, the result of a is -0.04, b is 0.09, substituting to Eq. (3) and Eq.(5), then

$$\varphi = \frac{1}{2\bar{\lambda}^2} [(0.96 + 1.09\bar{\lambda}^2) - \sqrt{(0.96 + 1.09\bar{\lambda}^2)^2 - 4\bar{\lambda}^2}] \quad (6)$$

As the consequence, Eq.(6) has a better corresponding with the test data than Eq.(2). The calculated results of Eq.(2) and Eq.(6) and the test data are illustrated in Figure 4. It can be seen that Eq.(2) may over-estimated the buckling load of the members with the smaller slenderness ratio so as to acquired a unsafe design. Therefore, Eq.(6) should be used to determined the stability factor of the FRP members. If the calculated result of φ is greater than 1.0, it should be equal to 1.0, which means the pipe may be crushed before buckling.

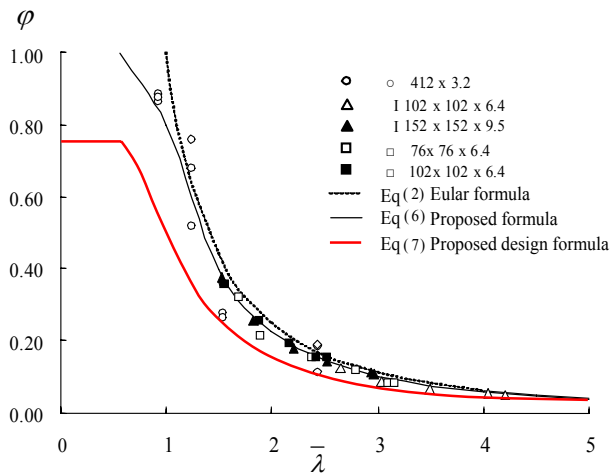


Figure 4. Stability factor curve of FRP member under axial compression

Eq.(6) is a fitting mean curve based on the tests data. For the practical design, a reduction coefficient ϕ_c should be multiplied on the results of Eq.(6), . If the guarantee rate is 97.72%, that is $\phi_c = 1/(\text{Mean} + 2 \cdot \text{Mean-square Deviation})$, its value can be determined by the tests data, which is about 0.75. So the following formula for design is proposed,

$$\varphi = \frac{3}{8\lambda^2} [(0.96 + 1.09\bar{\lambda}^2) - \sqrt{(0.96 + 1.09\bar{\lambda}^2)^2 - 4\bar{\lambda}^2}] \leq 0.75 \quad (7)$$

5 CONCLUSIONS

(1) It is shown in the axial loading test of five short GFRP pipes that they have the characteristics of linear elastic and brittle failure. And the dispersion of the compressive strength of GFRP is considerable, the maximum variation coefficient reaches 20%, but the dispersion of its elastic constant is smaller relatively as its variation coefficient is within 6%.

(2) Based on the experimental study of long GFRP pipes with the different slenderness ratio, the relationships of axial load to lateral displacement, vertical displacement and strain are obtained. It was found that the pipes with smaller slenderness ratio can be compressed to fracture at the ultimate compressive strain caused by lateral deformation after buckling, whereas, the pipes with larger slenderness ratio buckle in elastic and fail in oversize deformation.

(3) Based on the test results in this paper and literature, a stability factor formula of GFRP members under axial compression is presented, in which the initial defect and eccentricity are considered. And a calculation method for design is proposed.

6 ACKNOWLEDGEMENTS

The authors are grateful to the Natural Science Foundation of China for their support to the research presented here through a national key project (Project No. 50238030).

7 REFERENCE

- Barbero, E. J., and Raftoyiannis, I. G. 1993. Euler buckling of pultruded composite columns. *Composite Structures*, 1993, 24(2): 139-147.
- Barbero, E. J., and Tomblin, J. 1994. A phenomenological design equation for FRP columns with interaction between local and global buckling. *Thin-Walled Structures*, 18(2): 117-131.
- Berthelot, J-M. 1999. *Composite Materials: Mechanical Behavior and Structural Analysis*, Translated by Cole J M. New York: Springer-Verlag.
- Chen, J. 2003. *Stability of Steel Structures: Theory and Design*. Beijing: Science Press. (In Chinese)
- Goodman, J. W., and Gisksman, J. A. 1969. Structural evaluation of long boron composite column. *Composite Materials: Testing and Designing*, ASTM STP 460: 460-469.
- GB50018-2002. 2002. *Technical Code of Cold-Formed Thin-Wall Steel Structures*.
- Hewson, P. J. 1978. Buckling of pultruded glass fibre-reinforced channel section. *Composites*, 9(17): 56-60
- Lee, D. J., and Hewson, P. J. 1978. The use of fiber-reinforced plastics in thin-walled structures. In: Richards T H, Stanley P. eds. *Stability Problems in Engineering Structures and Components*. New York: Elsevier Applied Science, 23-55
- Shen, G. L. 1996. *Composites Mechanics*. Beijing: Tsinghua University Press. (In Chinese)
- Ye, L. P., and Feng, P. 2006. Applications and development of fiber-reinforced polymer in engineering structures. *China Civil Engineering Journal*, 39(3): 24-36. (In Chinese)
- Zhang, Y. L. 2003. *Handbook of Advanced Composites Manufacture Technologies*. Beijing: China Machine Press. (In Chinese)
- Zureick, A., Yoon, S., and Scott, D. 1992. Experimental investigation on concentrically loaded pultruded columns. In: Hamlin P, Verchery D. eds. *Proceedings of 2nd International Symposium of Textile Composites in Building Construction*. Paris, France, 207-215.
- Zureick, A., and Scott, D. 1997. Short-term behavior and design of fiber-reinforced polymeric slender members under axial compression. *Journal of Composites for Construction*, 1(4):140-149.